

ADVANCES IN FOREST FIRE RESEARCH

2022

Edited by

**DOMINGOS XAVIER VIEGAS
LUÍS MÁRIO RIBEIRO**

Turbulent Wildland Fire Spread by Ember Wash

Kevin Speer*^{1,2}; Bryan Quaife^{1,2}; Xin Tong^{1,2}

¹ Geophysical Fluid Dynamics Institute. Florida State University, Tallahassee, FL, 32306 USA,
{kspeer@fsu.edu}

² Department of Scientific Computing. Florida State University, Tallahassee, FL, 32306 USA,
{bquaife, xtong}@fsu.edu

*Corresponding author

Keywords

Fire-atmosphere interaction, rate-of-spread, ember wash, spotting, dynamics

Abstract

We implement an ember spotting and ember wash model within an idealized 2D coupled fire-atmosphere model. To do this, we add a stochastic transport to the background or total coupled wind field. An exponentially distributed or a normally distributed velocity anomaly added to the total wind vector represents a turbulent transport of the probability of ignition near ground by intermittent processes. These bed load transport processes may include including gusts, tumbling, and near-front small-scale coherent wind eddies that trap embers and transport them forward, hence carrying the fire along the near-surface total wind field.

1. Introduction

Short range spotting can be difficult to distinguish from fire front movement in higher winds, typical of strong spotting conditions. Some of this short range spotting is due to firebrands that did not rise in the fire's plume but rather spread nearly horizontally in the surface boundary layer. These and the heavier embers and burning debris that emerge from the main fire frontal region carried by strong winds are responsible for rapid movement and widening of the front. We use the phrase "*ember wash*" to denote this part of the fire.

Models have demonstrated the important role of plume intensity and turbulence in the degree and range of spotting, and suggested an exponential-like distribution of spotting downwind of the fire (Martin and Hillen, 2016; Bhutia et al., 2016). Data analyses confirm some aspects of this short-range behavior (Page et al., 2019; Storey et al., 2021). A possible example of this behavior appears in the "Northwest Oklahoma Fire Complex" of three large wildfires that burned about 800,000 acres in Oklahoma and Kansas (Figs. 1 and 2).

Our objective is to represent in an idealized fashion some of the most important processes for surface wind-driven fire in a turbulent flow. We show below how complex fire fronts and effects emerge from the interaction of background wind, fire-induced flow, and a new ember wash effect near intense fires.

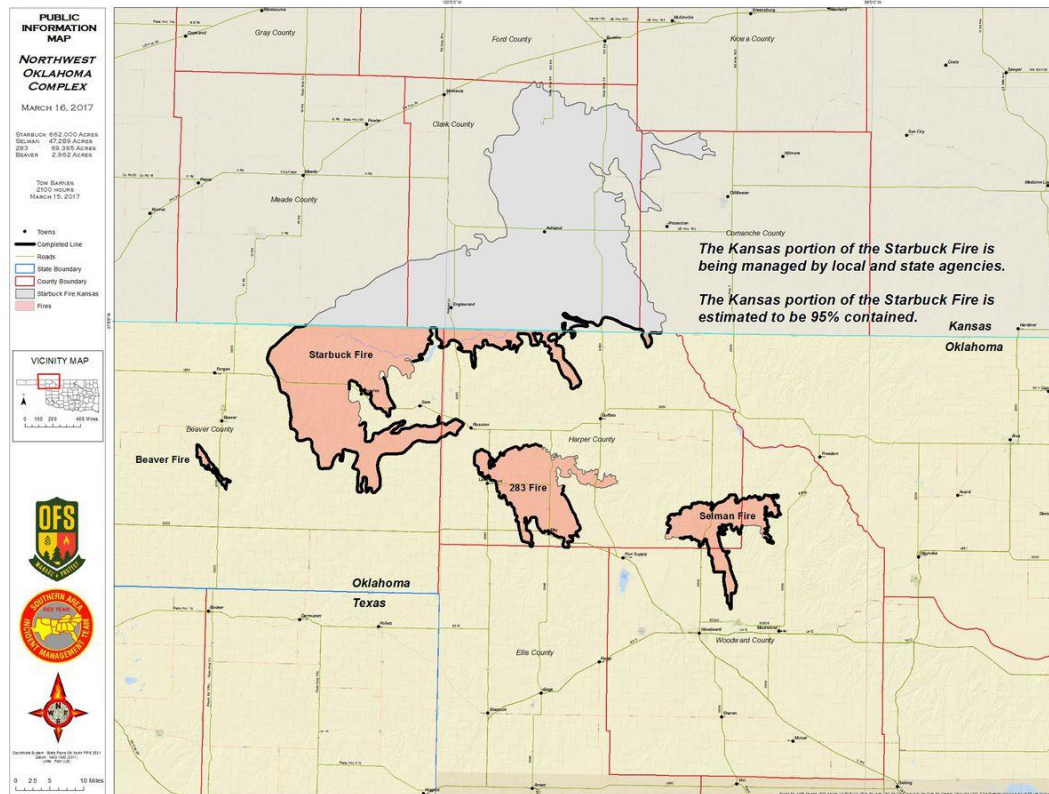


Figure 1- The 2017 NW Oklahoma Complex Fire consisted of several major fires and burned over 834,000 acres. Wind speeds were over 30 mph (15 m/s) with gusts up to 50 mph (25 m/s) in places. Source: Public Information Map of the OK Forest Service.

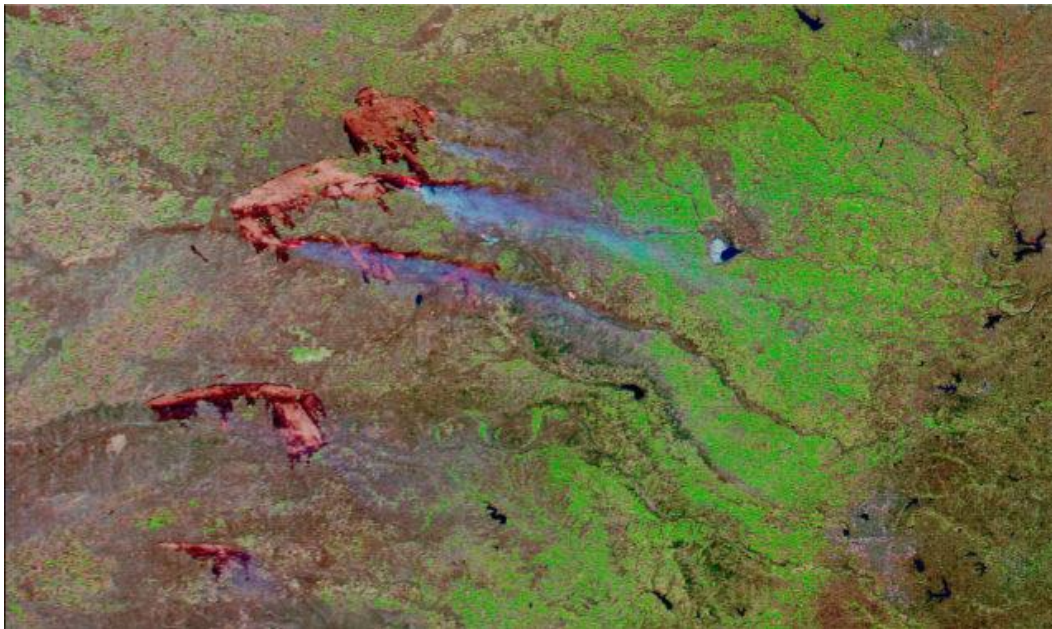


Figure 2- Infrared imagery of the 2017 NW OK Complex Fire near Woodward showing the intense fingering and complex spread behavior, some associated with wind and fuel variations and river drainage slopes. Flame heights were reported in places at over 40 ft.

2. Idealized Surface Wind Model

We use an idealized 2D model for near-surface wind in the presence of fire to investigate ember-enhanced spread in the presence of fire-atmosphere interaction (Quaife and Speer, 2021). The divergent flow is induced

by the rising buoyant fire plume that entrains surrounding air, and the rotational flow at the surface is induced by the lifting of horizontal background vorticity by the buoyant plume. Turbulent diffusion is incorporated into fire spread to represent the fluctuations in hot gases and flames at the near-surface boundary due to small-scale horizontal turbulent motion of the wind within and above the fuel. QS2021 provided a suite of runs that demonstrate various effects of fire-atmosphere interactions on spread rate and geometry of the fire. Standard phenomena such as a parabolic fire front shape, accelerated merging of flank fires, fingering, and other effects are well represented in the idealized model. In QS2021 the *first arrival time* or *time-of-arrival* heat map was emphasized as well as the rigorous relationship between this map and the rate-of-spread in any direction.

We solve for the flow generated by each burning elemental cell in a cellular automata (CA) model of combustion. A simple combustion term with fixed burn time is used. In the CA framework, we specify small-scale divergence and vorticity sources to the flow around individual fire elements which sum to produce the total wind on the fire front.

2.1. Solution Method

The model CA domain is defined by a two-dimensional rasterized grid and solved by decomposing the velocity into the sum of an irrotational and a solenoidal velocity field (Quaife and Speer, 2021). The first component is a background velocity that we take to be the uniform velocity U_{BG} . The other two velocity components are fire-induced, arising from flow convergence into the fire plume and from specified vorticity sources. Hilton et al 2018 call the divergent component the *pyrogenic potential*. At the flanks of the fire, we impose a vorticity source that, depending on the intensity of the fire, may be clockwise or counterclockwise on the fire flank. The model and velocity fields with and without the vorticity model are illustrated in Fig. 2.

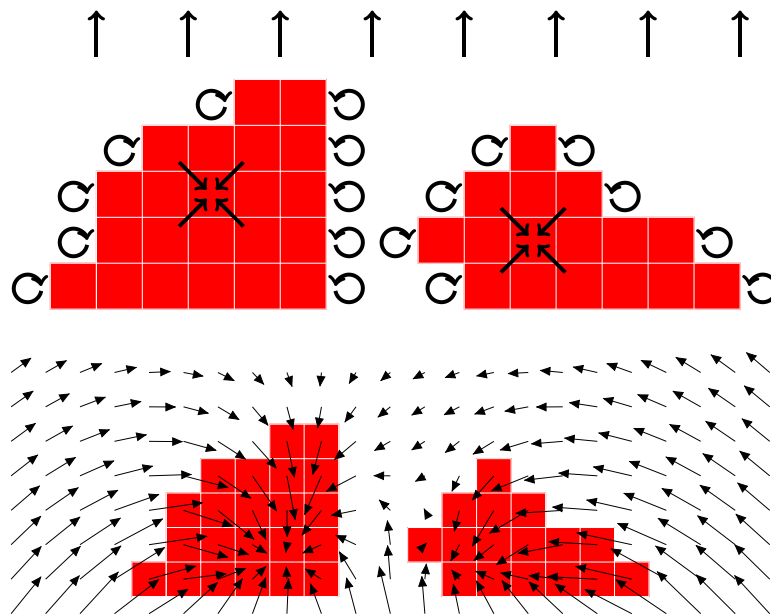


Figure 3- Wind around combustive elements (indicated by red cells). The atmospheric velocity is the sum of three components: a background flow, a pyrogenic potential or divergent term, and vorticity along the flanks.

Computing the flow field requires solving the two-dimensional Poisson equation with a known (and evolving) forcing function. We use the standard second-order central difference formula to discretize the Laplacian, and we impose a constant Neumann boundary condition. The resulting sparse linear system is solved with Matlab's backslash operator. With the total velocity field in hand, new cells must be ignited downwind. We use Bresenham's line algorithm to carry the fire downwind. This algorithm is a line drawing algorithm that determines cells of a rasterized geometry that are between a start and end point. We modify the algorithm since we only have a starting point at a burning cell and wind speed and direction. In addition, we stop igniting cells along the line if it reaches a cell that is either combusting or has no remaining fuel.

2.2. Model Configuration

Here, the cell size is 1m on a side, and the time evolution occurs over minutes to hours. The full model domain is rectangular, flat, and 200 m on a side. The only fuel parameter in the model is a constant burn time. This

parameter depends on the fuel and combustion process and is regarded here as an observed parameter, estimated from observations (Currie et al., 2018). While the range of this quantity can be large, mean values of a few seconds to minutes are typical in light to moderate fuels. The strength of the pyrogenic source is related to fire intensity by standard plume scaling.

We introduce a stochastic term that allows cells to ignite neighboring cells the time step before the original cells extinguish, with a probability of 0.4. This diffusion-based ignition occurs independently of the convection-based ignition due to wind. The rate of spread under diffusion is simply related to the burn time and probability of ignition since the model waits for the cell to burnout before igniting a neighboring cell.

The wind in our CA model is kinematic, and satisfies mass conservation but not a full set of momentum equations. Its role is to act as a "convective agent" for the probability of fire in a cell, and the added stochastic terms are designed to reflect the statistics of a multitude of processes and interactions in the surface boundary layer ahead of the fire front. In this implementation we relax this assumption and carry the fire stochastically down the local wind direction to simulate short-range spotting and ember wash.

3. Extension to Ember Spotting Effects

We extend this model with simple spotting and ember wash representations. We first consider an idealized spotting model to illustrate how embers may be distributed down the ambient wind when they are lofted, and the resulting flow complexity induced by the fire. Next we introduce *ember wash* that is induced by ember transport down the local near-surface wind. Representation of the latter is substantially different from spotting since the embers may roll or bounce along the ground as well as be carried by the wind hence their transport is more complicated, but also more localized to the fire front.

Spot fires are introduced based on a Gaussian-distributed lifetime (Tohidi and Kaye, 2017) with mean 20s and standard deviation 5s downwind *using the background flow* (not the total wind which include fire-induced flow). The reason for this is that aloft the main influence on trajectories is the background wind, with the plume effects secondary once the embers have been released by the plume into the surrounding environment. The ignition probability of the spot is given by a Poisson process with Bernoulli distribution and probability $p=0.01$. Higher probabilities produce too much fire with new fronts emerging rapidly mirroring the initial front; lower probabilities produce infrequent spotting. This is a useful idealization of the overall spotting process that reflects actual physical processes in an idealized manner. The subsequent spread of the fire is strongly influenced by the presence of spotting, which draws air in toward the new fire and dramatically changes the local flow (Fig. 4).

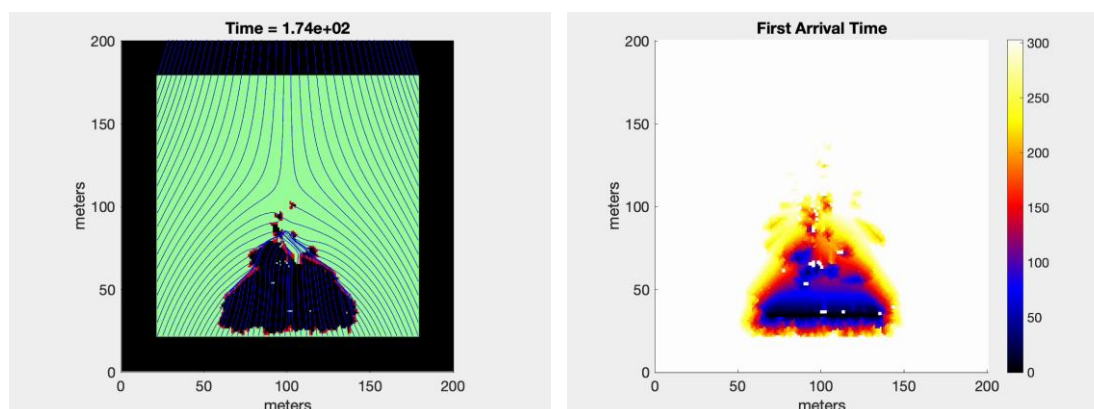


Figure 4- Idealized example of fire spread due to spotting. Fire progression map at 174s after ignition (left) and first arrival time heat map (right; seconds in color, with darker colors showing earlier arrival times). The addition of spot fires produces a complex fire-induced surface wind that affects subsequent spread. Streamlines of the wind (solid curves) indicate the interaction of a constant background wind of 1 m/s from the south (bottom) with the fire-induced wind; combusting elements are shown as red cells. The atmospheric velocity is the sum of three components: a background flow, a pyrogenic potential or divergent term, and vorticity along the flanks.

4. Extension to Ember Wash Effects

In contrast to spotting, *ember wash* or *ember blizzards* show a tendency for embers to spread near the surface rather than aloft. Much of this may occur in a tumbling or *bed load* mode of transport with embers bouncing, rolling, and being re-suspended and carried rapidly forward again in wind gusts. Thus we represent this process by a highly localized probability of ignition with an exponential decay away from the fire front. Such a shape may be justified as a subset of the observed close-range, exponential, spotting distributions in observations of spotting distance (Storey et al, 2021; Page et al, 2019) and sediment transport (Furbish and Schmeckle, 2020).

A dot-fire ignition pattern is used to generate a fire and illustrate the ember wash effect on spread (Fig. 5). To model the ember wash, the magnitude of the velocity of each burning cell is increased with a probability of $p=0.2$. The increase in magnitude is sampled from an exponential random variable with a mean of 1 m/s. Streamlines show the very different effect of fire-atmosphere interactions in the case of ember wash that produces a much stronger perturbation to the ambient wind due to the larger area on fire at any given time compared to a simpler continuous, front with a relatively narrow width. The combination of ember wash and fire-induced wind generates a spread geometry not well described by exponential alone from a single well-defined front. Intense fingering due to dynamics with ember wash can also enhance total spread rates. Interactions with structures will be described in our presentation.

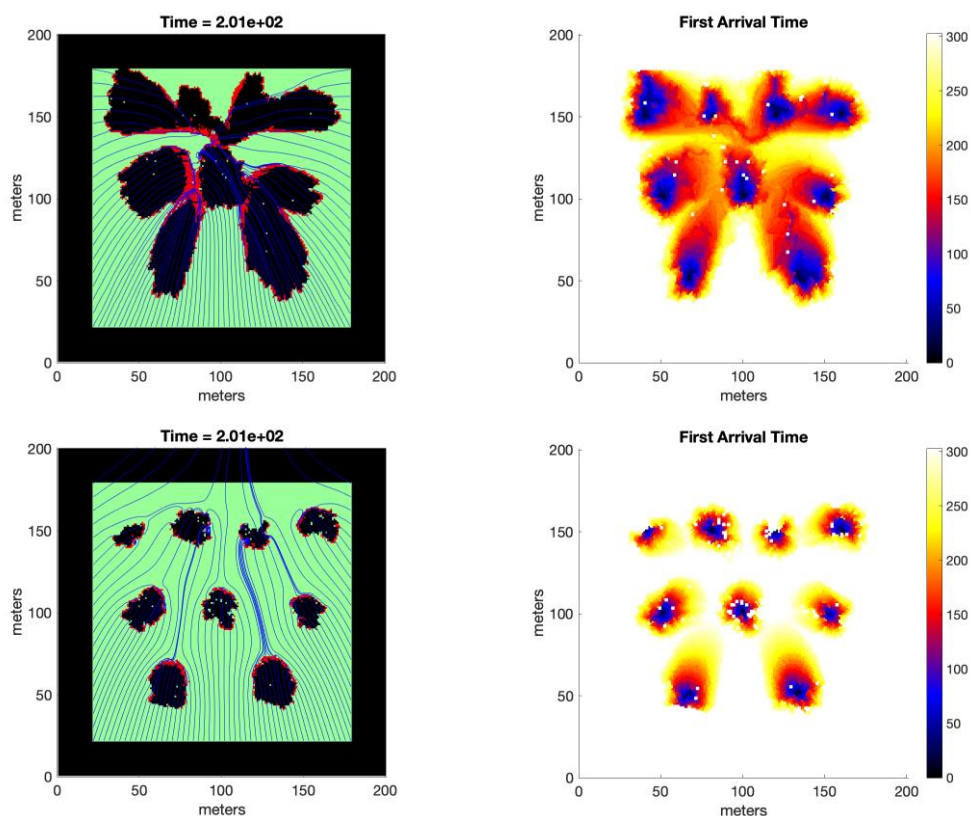


Figure 5- Fire spread with ember wash (top) and without ember wash (bottom). Fire progression map at 201s after ignition (left) and first arrival time heat map (right); seconds in color, with darker colors showing earlier arrival times. The ignition pattern is nine isolated spots. With ember wash a large region of ignition appears following the direction of the coupled fire-induced wind field. Streamlines of the wind (solid curves) indicate the interaction of a constant background wind from the south (bottom) with the fire-induced wind; combusting elements are shown as red cells. The atmospheric velocity is the sum of three components: a background flow, a pyrogenic potential or divergent term, and vorticity along the flanks.

5. References

Bhutia, Sangay, Mary Ann Jenkins and Ruiyu Sun, Comparison of Firebrand Propagation Prediction by a Plume Model and a Coupled-Fire/Atmosphere Large-Eddy Simulator J. Adv. Model. Earth Syst., 2(1), 2010.

- Currie, Miles, Kevin Speer, J. Kevin Hiers, Joe J. O'Brien, Scott Goodrick, and Bryan Quaife, Pixel-level statistical analyses of prescribed fire spread, *Can. J. For. Res.*, 49.1:18026, 2019.
- Albini Frank, A., Martin E. Alexander B, C, E and Miguel G. Cruz, A mathematical model for predicting the maximum potential spotting distance from a crown fire *International Journal of Wildland Fire*, 21:609–627, 2012.
- Furbish, D. J., and M. W. Schmeckle (2013), A probabilistic derivation of the exponential-like distribution of bed load particle velocities, *Water Resour. Res.*, 49, 1537–1551, doi:10.1002/wrcr.20074.
- Martin, Jonathan and Thomas Hillen, The Spotting Distribution of Wildfires, *Appl. Sci.*, 6(6):177, 2016.
- Page, Wesley G., Natalie S. Wagenbrenner, Bret W. Butler, and David L. Blunck, An analysis of spotting distances during the 2017 fire season in the Northern Rockies, USA, *Can. J. For. Res.*, 49:317–325, 2019.
- Quaife, Bryan, and Kevin Speer, A Simple Model for Wildland Fire Vortex-Sink Interactions, *Atmosphere*, 12(8):1014, 2021.
- Storey, Michael, A., Owen F. Price, Ross A. Bradstock, and Jason J. Sharples, Analysis of Variation in Distance, Number, and Distribution of Spotting in Southeast Australian Wildfires, *Fire*, 3(10), 2020.
- Tohidi, Ali and Nigel B. Kaye, Stochastic modeling of firebrand shower scenarios, *Fire Safety Journal*, 91:91-102, 2017.